OPTIMIZATION OF ARTIFICIAL VENTILATION THERAPY FOR ARDS BASED ON AUTOMATIC IDENTIFICATION OF LUNG PROPERTIES

H. Luepschen*, T. Meier**, M. Grossherr**, T. Leibecke*** and S. Leonhardt*

* Medical Information Technology, Helmholtz-Institute, RWTH Aachen University, Germany
** Department of Anaesthesiology, University of Lübeck, Germany
*** Department of Radiology, University of Lübeck, Germany

luepschen@hia.rwth-aachen.de

Abstract: This paper reports on the automation of the "open lung concept" (OLC) and discusses the benefits of electrical impedance tomography (EIT) in this context. The OLC is a ventilation strategy using lung recruitment maneuvers especially suited for patients with acute respiratory distress syndrome (ARDS). A fuzzy-logic based ventilation and monitoring expert system has been developed featuring an artificial ventilator, a fast EIT system, an online blood gas monitor, a capnograph, a patient monitor and a CT scanner trigger device. The invasively measured partial pressure of oxygen is fed back into a closed-loop fuzzy controller, which is part of a finite state machine that implements the different stages of the OLC. During that process, more than 20 hemodynamical, pulmonary and ventilatory parameters are quasi-continuously recorded. EIT, as well as, CT images are made. The results obtained show the feasibility of the approach and the potential of the supplementing EIT system to become a valuable bedside monitoring and control tool for advanced artificial ventilation strategies.

Introduction

The acute respiratory distress syndrome (ARDS) was first described in 1967 (1). It is a life-threatening state of the lung which is characterized by general pulmonary inflammatory reactions with a consecutive reduction of surfactant production (a substance reducing surface tension in the alveoli) and a capillary leakage syndrome. This leads to interstitial and alveolar lung edema. Thus, both the volume of the extravascular lung water and the lung weight rise, promoting the collapse of peripheral airways and lung parenchyma (atelectasis), mainly in the gravitationally dependent regions (2).

As a consequence of the reduced size of the lung ("baby lung", 3), lung compliance and diffusion capacity decrease, while right-to-left shunt increases resulting in a likewise increased respiratory effort and an impaired gas exchange (hypoxemia, hypercapnia) (4). State-of-the-art medical treatment includes artificial ventilation with increased fractions of inspired oxygen (FiO2) at low tidal volumes (V_T) and adequate positive end-expiratory pressures (PEEP) (5). Despite enormous research efforts, mortality rate among patients is still reported to be high (30%-50%) (5,6) which seems to be partly induced by artificial ventilation itself (volutrauma, barotrauma, atelectrauma) (7).

The amount of PEEP necessary, the influence of etiological category (8) as well as the significance and benefit of alveolar opening maneuvers (recruitment maneuvers, RM) to remove atelectasis are still controversially discussed (2,9-13). This might be partly due to the fact that comparability of the various studies is hard to assess (making reasonable deductions difficult) and, probably more important, that treatment of ARDS should become more specific, i.e. personalized, reflecting the individual patient's need (11). To achieve this goal, careful laboratory and bedside observations with standardized protocols will be required. At the same time, a large number of different parameters must be continuously examined which calls for a computer-aided approach.

For this reason, a fuzzy-logic based ventilation expert system has been developed and fed with carefully collected medical knowledge from experienced physicians. The system is capable of performing predefined RMs while continuously recording more than 20 hemodynamical, pulmonary and ventilatory parameters. In order to evaluate the setup and the feasibility of the approach, the system was programmed to conduct a particular recruitment scheme called the "open lung concept" (OLC, 14) and tested in porcine lavage models of respiratory failure. The OLC aims at reducing shear stress between aerated (i.e. open) and collapsed units of the lung, while maximizing partial pressure of arterial oxygen (PaO_2).

The ventilation and monitoring setup is supplemented by an electrical impedance tomograph (EIT) with a high temporal resolution. The EIT was evaluated not only in terms of its ability to visualize the recruitment procedure, but also in terms of its potential to provide control variables that may help to supersede the invasive PaO_2 measurement. Conventional computed tomography (CT) reference scans with high spatial resolution were concurrently made serving as a "gold standard". In fact, CT has already been proven useful for evaluating alveolar recruitment, however, it is static, radioactive, expensive and, therefore, not practical for routine use at bedside (15,16). EIT might have the potential to bridge that gap and to become a valuable bedside monitoring and control tool for advanced artificial ventilation strategies.

ISSN: 1727-1983

Background

The basis of all ventilation strategies using RMs (like the OLC) is the fact that the relationship between lung pressure and lung volume is nonlinear (hysteresis of the P-V curve) which is particularly pronounced in lungs suffering from ARDS. This feature results from collapsed parts of the lung which need to be reopened by increased airway pressures and, subsequently, remain open at lower pressures (17).

As the PaO_2 is correlated with the size of the diffusion area in the lung, the described hysteresis is even more distinct in the P-PaO_2 curve of ARDS lungs, see figure 1.

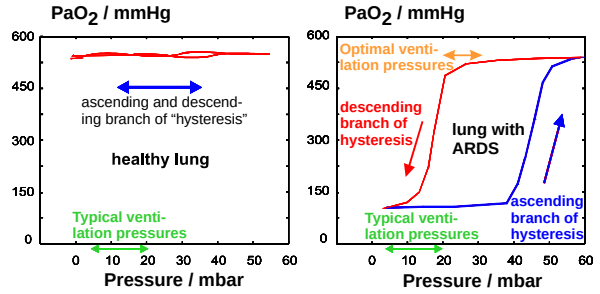

Figure 1: Distinct P-PaO_2 hysteresis of a porcine ARDS lung (right) compared to a more or less hysteresis-free healthy lung (left) at FiO_2 = 100%

The optimal operation point for ventilation of such an ARDS lung would be at the highest PaO_2 ("open lung") with the lowest possible pressure settings, i.e. at the top left of the descending branch of hysteresis. In order to identify these optimal ventilation settings, it is necessary to carefully titrate the lung opening and closing ventilation pressures PIP_{open} (peak inspiratory pressure) and $PEEP_{close}$ by cycling through the complete loop of hysteresis (figures 1 and 2) (18).

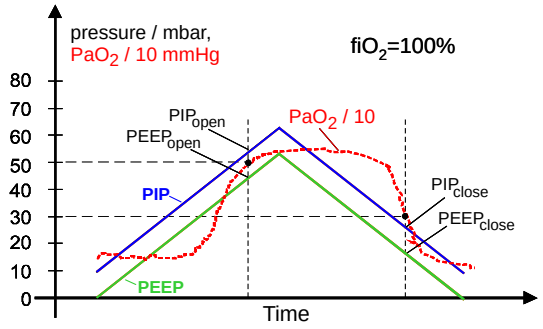

Figure 2: Identification of the large-signal P-PaO_2 behavior of an ARDS lung and of the opening/closing pressures

Materials and Methods

Animal experiments: The study was performed in collaboration with the University of Luebeck, Germany, and approved by the local animal ethics committee. Three female domestic pigs (25-28 kg) received premedication, general anesthesia, intubation and were moved to the radiology department. After adding a muscle relaxant, multiple lung lavages with isotonic saline solution at 37°C were conducted inducing atelectasis and lung edema, in order to simulate patients with acute respiratory distress syndrome (ARDS). Surfactant depletion was carried out until PaO_2 stayed below 100 mmHg for at least 15 minutes. Afterwards, ventilator settings were kept stable for one hour before running the automated OLC ventilation scheme.

Ventilation and monitoring setup: The ventilation and monitoring setup "VentiLab" consists of a medically approved Panel PC (POC-153, Advantech Co., Ltd.), an electrically controllable ventilator (Servo 300, Siemens-Elema), an online blood gas monitor with a Paratrend 7+ sensor (TrendCare Satellite, Diametrics Medical Inc.), a patient monitor (Sirecust 1281, Siemens), a capnograph (CO_2SMO+, Respironics, Inc.) and an electrical impedance tomography prototype system (EIT evaluation Kit, Fa. Draeger medical, Luebeck / GoeMF II system, University of Goettingen), see figure 3. CT scans were made triggering an Aquilion 4 system (Toshiba Corp.).

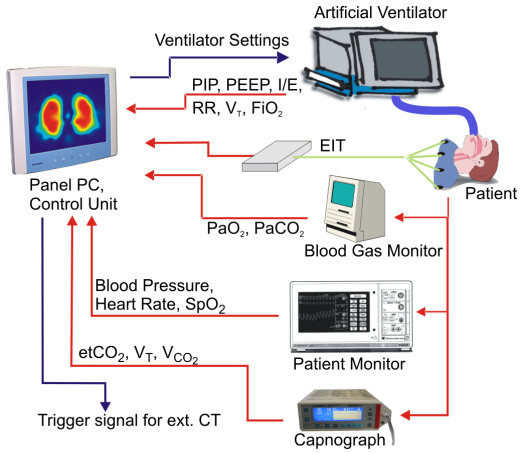

Figure 3: Ventilation and monitoring setup "VentiLab" featuring sensor fusion and automatic ventilation control

The Panel PC has a PCI Analog-to-Digital Converter (ADC) card to read pressure and flow values of the artificial ventilator at a sampling rate of 100 Hz. Additionally, an 8-channel PCI Digital-to-Analog Converter (DAC) card is used for setting PIP, PEEP, inspiration to expiration ratio (I:E), respiratory rate (RR) and FiO_2, and for creating the CT trigger signal. EIT data is received via an USB interface. All other parameters are read using standard RS232 connections. Programs were written with the graphical programming tool LabVIEW® (National Instruments Corp.).

Electrical impedance tomography: EIT is a method to determine the spatial impedance distribution in a body cross section. N electrodes (here: N = 16) are equidistantly attached to the skin around the subject's thorax. It can be shown that $M=(N*(N-3)/2)$, i.e. M=104 independent transfer impedance measurements can be made. For that reason, all adjacent electrodes are sequentially supplied with a small alternating current (e.g. 5 mA_{rms} @ 50 kHz) using a DAC while measuring

ISSN: 1727-1983

the transfer voltages at the (*N*-3) remaining electrode pairs with an ADC, see figure 4.

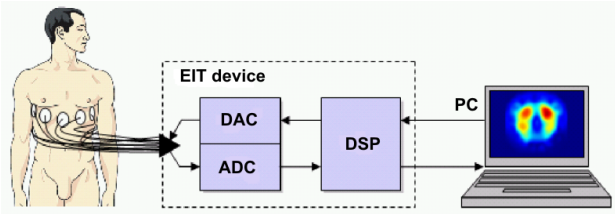

Figure 4: Principle of EIT measurements around the thorax (DSP = Digital Signal Processor)

A row vector g_n with 104 rows is created at a rate of 13 frames per second (frame number *n*) containing the transfer voltages. The corresponding EIT image vector z_n can be reconstructed by solving an ill-posed, nonlinear inverse problem. In this case, a classic back-projection algorithm with a matrix *B* (dim 912x104) is used (19,20).

To obtain better EIT imaging results and to avoid having to take into account the shape of the subject's 3-D body, only the changes in tissue impedance and not absolute values are considered. The appropriate relative row vector dg_n is gained from a comparison with a reference vector g_{ref}. Consequently, the associated *difference* EIT (dEIT) image vector dz_n is given by:

$$dz_n = B \cdot dg_n \tag{1}$$

The *functional* EIT (fEIT) $f_{n,m}$ image vector can be calculated as the standard deviation for each pixel *p* of a series of *m* consecutive dEIT images (21):

$$f_{n,m}(p) = \sqrt{\frac{\sum_{k=n-m+1}^{n}[dz_k(p) - \overline{dz_{n,m}}(p)]^2}{m-1}} \tag{2}$$

with

$$\overline{dz_{n,m}}(p) = \frac{\sum_{k=n-m+1}^{n} dz_k(p)}{m} \tag{3}$$

The resulting image provides a steady-state description of a usually periodical physiological process (here: regional lung ventilation with m = 260, i.e. 20 seconds). In addition, a global impedance value G_n can be calculated by simply summing up all pixel values of the dEIT image vector dz_n, giving a good measurement of global lung volume (22).

$$G_n = \sum_{p=1}^{912} dz_n(p) \tag{4}$$

Fuzzy controller: Patients are divided into three groups (patients with light, medium and severe forms of ARDS). For each group, fuzzy controllers were implemented to find the opening and closing pressures, using the fuzzy toolbox fuzzyTECH® (INFORM GmbH, Germany) fed with expert knowledge from experienced physicians (more than 50 "if … then" rules) (18). The resulting six fuzzy controllers are part of a finite state machine which handles the four different phases of an OLC recruitment maneuver: "opening" (phase 1), "closing" (phase 2), "re-opening" (phase 3) and "steady-state" (phase 4), see figure 5.

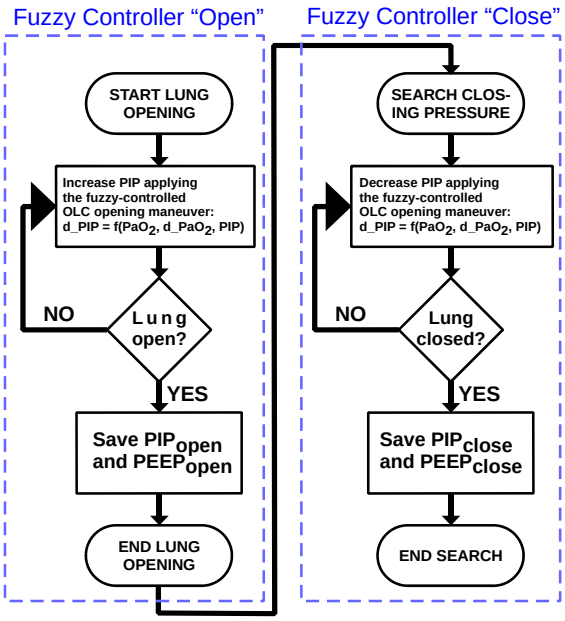

Figure 5: Phase 1 and phase 2 of the flow chart for the finite state machine. The opening and closing pressures are carefully titrated using pressure-control ventilation mode (PCV). Not shown: Re-opening of the lung and steady-state ventilation.

During the opening phase, PIP is stepwise increased until the lung is supposed to be open (i.e. the lu_open status variable becomes larger than 0.5). The calculated increment of PIP (d_PIP) depends on PaO_2, its gradient (d_PaO_2) and the actual PIP itself (figure 6).

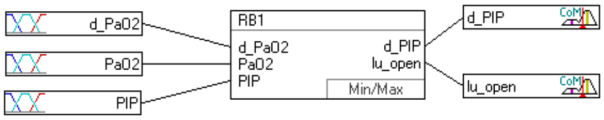

Figure 6: Inputs and outputs of each fuzzy controller. PIP is changed based on PaO_2, its gradient (d_PaO_2) and the actual PIP itself: PIP(k+1) = PIP(k) + d_PIP. If lu_open > 0.5, the lung is supposed to be open.

To determine the output variables d_PIP and lu_open, the "crisp" absolute input variables are first mapped to linguistic fuzzy variables by sets of membership functions known as fuzzy sets ("fuzzification"). Then, each appropriate "if … then" rule is invoked and the results are combined applying the "max-min" inference method. Finally, the combined result is converted back into the specific crisp output

ISSN: 1727-1983

variables using "centroid defuzzification". The 3-D shaded surface plots of the fuzzy controller for the opening maneuver in patients with light forms of ARDS can be seen in figure 7 (d_PIP over PaO_2 and d_PaO_2) and figure 8 (lu_open over PaO_2 and d_PaO_2) at a fixed PIP of 30 cmH_2O.

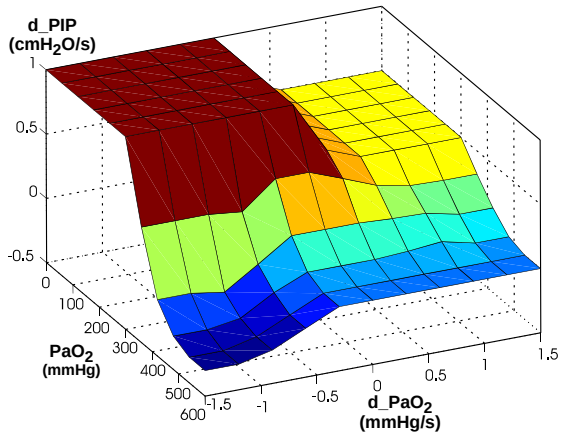

Figure 7: 3-D shaded surface plot of d_PIP over PaO_2 and d_PaO_2. (fixed PIP = 30 cmH_2O and FiO_2 = 100%, opening controller for patients with light forms of ARDS).

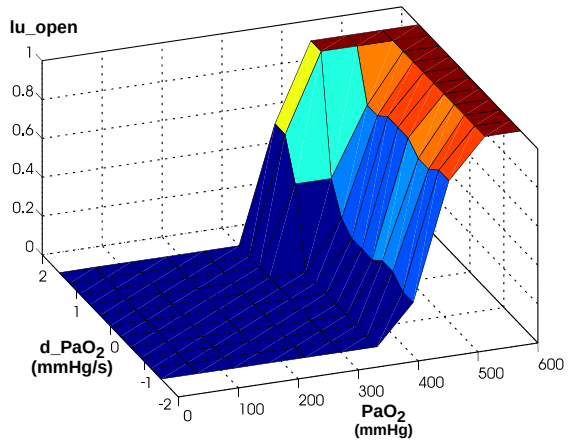

Figure 8: 3-D shaded surface plot of the lung open indicator lu_open over d_PaO_2 and PaO_2 (fixed PIP = 30 cmH_2O and FiO_2 = 100%, opening controller for patients with light forms of ARDS). Lung is considered to be open if lu_open > 0.5.

During the closing phase, a similar fuzzy controller is used to find PIP_{close} and $PEEP_{close}$ at the inflection point of the upper branch of hysteresis (figure 1). Then, the lung is reopened for 12 breath cycles with the previously found PIP_{open} and $PEEP_{open}$ and ventilated in the steady-state phase by setting the PEEP level 2 cmH_2O above the found $PEEP_{close}$.

Results and Discussion

The pulmonary parameters during an automated, fuzzy-controlled OLC maneuver conducted in a porcine lavage model of ARDS can be seen in figure 9. The corresponding G_n curve is shown in figure 10.

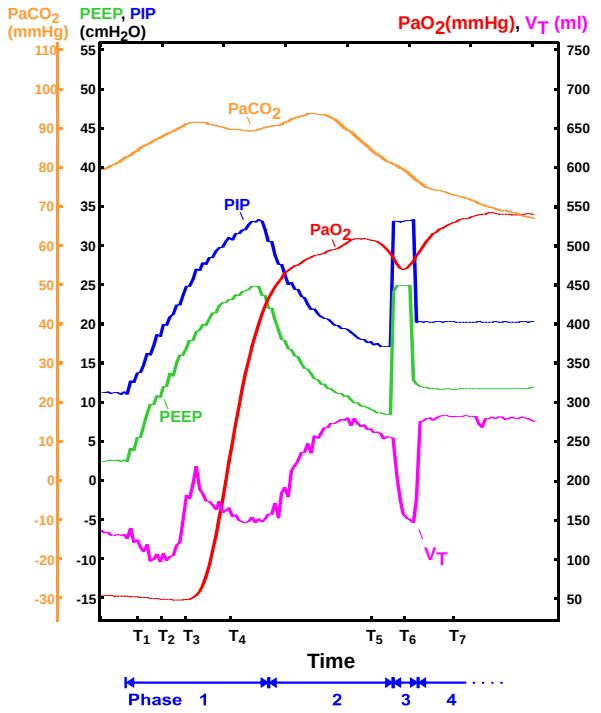

Figure 9: Pulmonary parameters during an OLC maneuver.

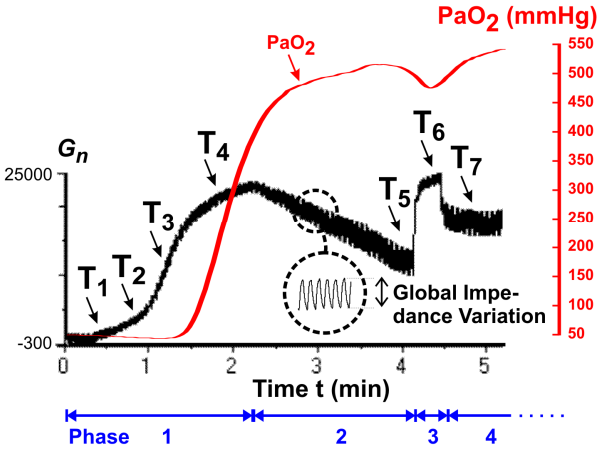

Figure 10: Four phases of the fuzzy-controlled OLC maneuver (opening, closing, re-opening and steady-state).

In the opening phase (phase 1, times T_1-T_4), PEEP and PIP are synchronously increased leading to a similarly increasing global impedance G_n, as expected. Tidal volume V_T remains rather small, which can also be deduced from looking at the global impedance variation (or tidal variation) of the G_n curve (23). PaO_2 starts to rise as soon as PIP and PEEP exceed a certain level. In this case, this is roughly at PIP = 20 cmH_2O. The lung is identified as being open when PaO_2 reaches "healthy" values above 400 mmHg and d_PaO_2 is still positive (shortly after time T_4). Looking at the slope of the envelope of the G_n curve, it seems reasonable to assume that the opening pressure PIP_{open} was found by the fuzzy controller a little bit too late. This might be due to the dynamic latency (>= 15 sec) of the online PaO_2 measurement. It has to be further investigated if the ventilation pressure used at the upper inflection

ISSN: 1727-1983

point of the G_n between T_3 and T_4 would have been sufficient to recruit the lung.

In the closing phase (phase 2), PIP and PEEP are decreased until the PaO_2 curve starts to indent (time T_5). Looking again at the G_n curve, a clear indication of a serious lung collapse is not visible at this point. Therefore, it might be possible that the closing pressure $PEEP_{close}$ was found too early because of the high sensitivity of the underlying fuzzy controller, an assumption that also has to be further investigated.

After a successful re-opening (phase 3, time T_6), steady-state ventilation (phase 4) is started with an associated sustained decrease of arterial carbon dioxide partial pressure ($PaCO_2$) and PaO_2 values in excess of 500 mmHg. Tidal volumes (V_T) are around 280 ml (approximately doubled compared to phases 1 and 3).

After 16 minutes of steady-state ventilation, the fuzzy controller was switched off and PEEP manually decreased by 1.5 cmH_2O (t = 17 min, figure 11).

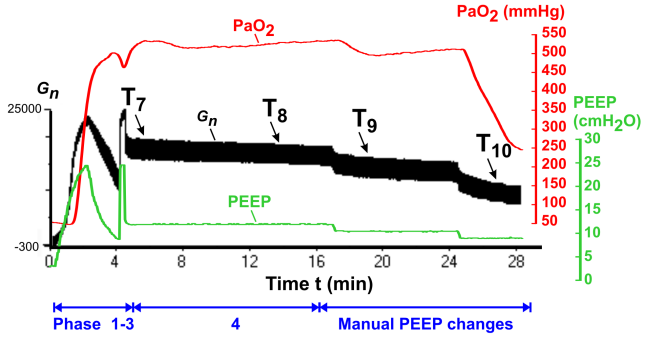

Figure 11: All phases of the fuzzy-controlled OLC (1-4) and the following manual PEEP changes.

At the second manual PEEP reduction (t = 24 min) of *only* 1 cmH_2O, G_n and especially PaO_2 immensely break away, a clear sign of derecruitment. This impressively demonstrates the difficulty in finding and preserving the proper PEEP level and might explain the poor results of lung recruitment maneuvers regarding sustained improvement of PaO_2 in a recent study (24).

In figure 12, CT scans and fEIT, as well as, dEIT images can be seen at all relevant times T_1-T_{10}. It has to be kept in mind that EIT actually provides a real-time stream of images (here: 13 images per second) and that the images shown display only a snap-shot of the whole process. The auto-scaled fEIT images show the ventilation distribution in the examined pig lungs, where red areas are more ventilated than green or blue areas. The fixed-scaled end-inspiratory dEIT images give an impression of the PIP and PEEP levels used and the amount of distension of the different lung regions.

Looking at time T_1, the CT scan indicates that large parts of the dorsal lung are collapsed and do not participate in gas exchange. This observation is in good accord with the associated fEIT image which depicts ventilation only in the ventral regions 1 and 3.

Increasing PIP and PEEP (figure 12: T_2, T_3) removes atelectasis, initiates a more evenly distributed ventilation and shifts ventilation to the more dorsal regions 2 and 4.

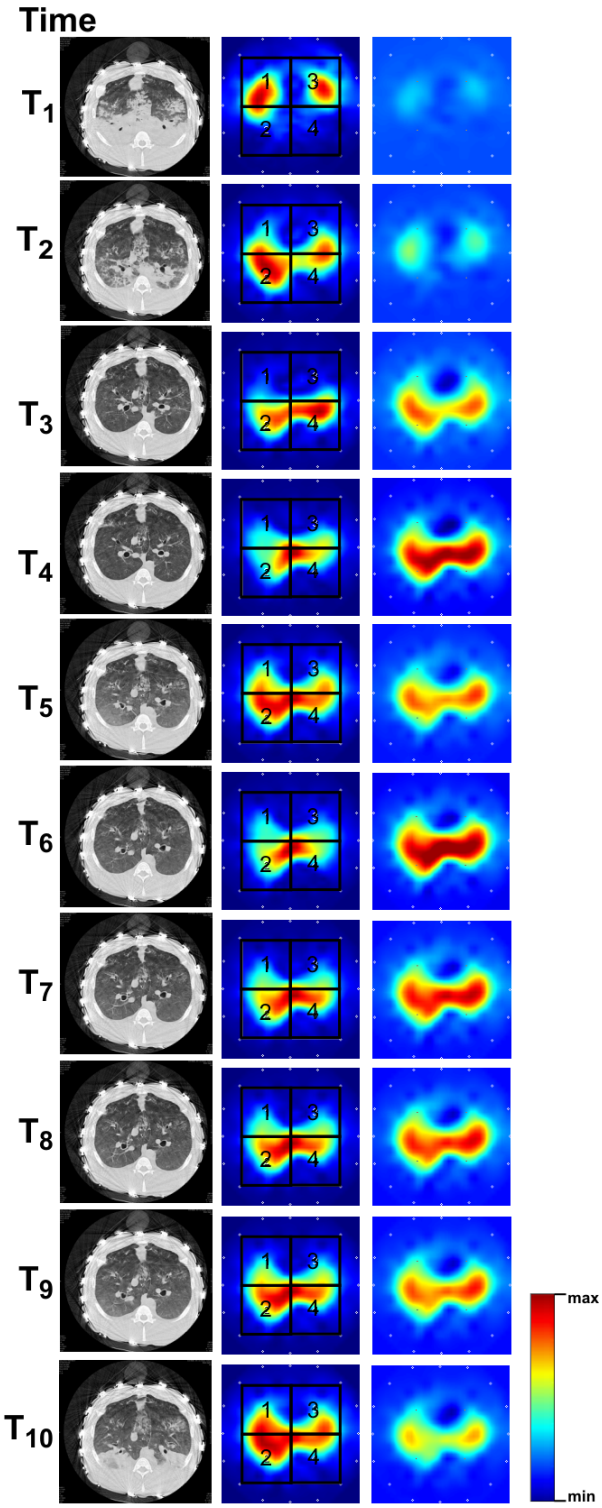

Figure 12: CT images (left), auto-scaled fEIT images (middle) and fixed-scaled end-inspiratory dEIT images (right) at all relevant times T_1-T_{10}.

This leads to an enormous increase in PaO_2 at the same time (figure 9: T_1-T_4). At times T_4 and T_6, the fEIT images show that ventilation is mainly concentrated between regions 2 and 4, another indicator that the opening pressure PIP_{open} was found too late by the fuzzy controller. At time T_{10}, after manually decreasing PEEP the second time, the CT scan again

ISSN: 1727-1983

depicts atelectasis in the dorsal regions of the lung, ventilation is less homogeneously distributed and shifted upwards towards regions 1 and 3, an effect of derecruitment.

Conclusions and Acknowledgements

An automatic fuzzy-logic based ventilation and monitoring expert system has been presented and successfully tested in animal experimental studies. The system is capable of performing predefined recruitment maneuvers and demonstrated to improve PaO_2 for a prolonged period of time. In addition, $PaCO_2$ was significantly reduced and collapsed regions of the lung were successfully re-opened. There is no statistical data on the outcome of this therapy as of yet, but the presented results are promising so far.

The supplementing EIT system showed a high potential to visualize and assess recruitment of the lung and to assist advanced ventilation strategies.

The support of E. Teschner, Fa. Draeger medical, Luebeck, is gratefully acknowledged.

References

[1] ASHBAUGH D. G., BIGELOW D. B., PETTY T. L., LEVINE B. E. (1967): 'Acute respiratory distress in adults', *Lancet*, **2**, pp. 319-323

[2] BARBAS C.S., DE MATOS F.J., PINCELLI M.P., ET AL (2005): 'Mechanical ventilation in acute respiratory failure: recruitment and high positive end-expiratory pressure are necessary', *Curr Opin Crit Care*, **11**, pp. 18-28

[3] GATTINONI L., PESENTI A. (2005): 'The concept of "baby lung" ', *Intensive Care Med*, **31**, pp. 776-784

[4] GATTINONI L., PESENTI A. (1991): 'Computed tomography scanning in acute respiratory failure', in ZAPOL W.M., LEMAIRE F. (Eds): 'Adult Respiratory Distress Syndrome', (Marcel Dekker, New York), pp. 199-221

[5] ARDS CLINICAL TRIALS NETWORK (2000): 'Ventilation with lower tidal volumes as compared with traditional tidal volumes for acute lung injury and the acute respiratory distress syndrome', *N Engl J Med*, **342**, pp. 1301-1308

[6] ARTIGAS A. (1998): 'Prognostic Factors and Outcome of ALI', in MARINI J.J., EVANS T.W. (Eds.): 'Acute Lung Injury (Update in intensive care and emergency medicine: 30)', (Springer-Verlag, Berlin, Heidelberg), pp. 16-38

[7] MOLONEY E.D., GRIFFITHS, M.J.D. (2004): 'Protective ventilation of patients with acute respiratory distress syndrome', *Br J Anaesth*, **93**, pp. 261-270

[8] LIM C.M., JUNG H., KOH Y., ET AL (2003): ,Effect of alveolar recruitment maneuver in early acute respiratory distress syndrome according to antiderecruitment strategy, etiological category of diffuse lung injury, and body position of the patient', *Crit Care Med*, **31**(2), pp. 411-418

[9] ARDS CLINICAL TRIALS NETWORK (2003): 'Effects of recruitment maneuvers in patients with acute lung injury and acute respiratory distress syndrome ventilated with high positive end-expiratory pressure', *Crit Care Med*, **31**(11), pp. 2592-2597

[10] MARINI J.J. (2003): 'Are recruiting maneuvers needed when ventilating acute respiratory distress syndrome?', *Crit Care Med*, **31**(11), pp. 2701-2703

[11] DRIES D.J., MARINI J.J. (2002): 'A Rationale for Lung Recruitment in Acute Respiratory Distress Syndrome', *J Trauma*, **54**(2), pp. 326-328

[12] CROTTI S., MASCHERONI D., CAIRONI P., ET AL (2001): 'Recruitment and derecruitment during acute respiratory failure: a clinical study', *Am J Respir Crit Care Med*, **164**, pp. 131-140

[13] SLUTSKY A.S., RANIERI V.M. (2000): 'Mechanical ventilation: lessons form the ARDSNet trial', *Respir Res*, **1**(2), pp. 73-77

[14] LACHMANN, B. (1992): 'Open the lung and keep the lung open', *Intensive Care Med*, **18**, pp. 319-322

[15] KUNST P.W., DE ANDA G.V., BOEHM S.H., ET AL (2000): 'Monitoring of recruitment and derecruitment by electrical impedance tomography in a model of acute lung injury', *Crit Care Med*, **28**(12), pp. 3891-3895

[16] GATTINONI L., PESENTI A., AVALLI L., ET AL (1987): 'Pressure-volume curve of total respiratory system in acute respiratory failure: computed tomographic scan study', *Am Rev Respir Dis*, **136**, pp. 730-736

[17] BOEHM S., LACHMANN B. (1996): 'Pressure-control ventilation – putting a mode into perspective', *J Intensive Care*, **3**, pp. 12-27

[18] LEONHARDT S., BOEHM S. (1999): 'Control methods for artificial ventilation of ARDS patients', Proc. of EMBEC 1999, Vienna, Austria

[19] BARBER D.C., BROWN B.H., FREESTON I.L. (1983): 'Imaging and spatial distributions of resistivity using applied potential tomography', *Electronics letters*, **19**, pp. 93-95

[20] LEONHARDT S., MEIER T., GROSSHERR M., ET AL (2004): 'Validation and clinical potential of thoracic electrical impedance tomography', Proc. of Biomedizinische Technik, Ilmenau, Germany, **49**(2), pp. 146-147

[21] HAHN G., SIPINKOVA F., BAISCH F., HELLIGE G. (1995): 'Changes in the thoracic impedance distribution under different ventilatory conditions', *Physiol Meas*, **16**(3A), pp. A161-A173

[22] WOLF G.K., ARNOLD J.H. (2005): 'Noninvasive assessment of lung volume: respiratory inductance plethysmography and electrical impedance tomography', *Crit Care Med*, **33**(2), pp. S163-S169

[23] LUEPSCHEN H., MEIER T., GROSSHERR M., ET AL (2005): ,Clinical applications of thoracic electrical impedance tomography', Proc. of 6th Conference on Biomedical Applications of Electrical Impedance Tomography, London, UK, June 22-24, 2005

[24] ARDS CLINICAL TRIALS NETWORK (2003): 'Effects of recruitment maneuvers in patients with acute lung injury and acute respiratory distress syndrome ventilated with high positive end-expiratory pressure', *Crit Care Med*, **31**(11), pp. 2592-2597

ISSN: 1727-1983